

A Truncation Error Analysis of Third-Order MUSCL Scheme for Nonlinear Conservation Laws

Hiroaki Nishikawa*

National Institute of Aerospace, Hampton, VA 23666, USA

Abstract

This paper is a rebuttal to the claim found in the literature that the MUSCL scheme cannot be third-order accurate for nonlinear conservation laws. We provide a rigorous proof for third-order accuracy of the MUSCL scheme based on a careful and detailed truncation error analysis. Throughout the analysis, the distinction between the cell average and the point value will be strictly made for the numerical solution as well as for the target operator. It is shown that the average of the solutions reconstructed at a face by Van Leer's κ -scheme recovers a cubic solution exactly with $\kappa = 1/3$, the same is true for the average of the nonlinear fluxes evaluated by the reconstructed solutions, and a dissipation term does not contribute to the leading third-order error. Finally, noting that the target spatial operator is a cell-averaged flux derivative, we prove that the leading truncation error of the MUSCL finite-volume scheme is third-order with $\kappa = 1/3$. The importance of the diffusion scheme is also discussed: third-order accuracy will be lost when the third-order MUSCL scheme is used with a wrong fourth-order diffusion scheme for convection-diffusion problems. Third-order accuracy is verified by thorough numerical experiments for both steady and unsteady problems. This paper is intended to serve as a reference to clarify confusions about third-order accuracy of the MUSCL scheme, as a guide to correctly analyze and verify the MUSCL scheme for nonlinear equations, and eventually as the basis for clarifying third-order unstructured-grid schemes in a subsequent paper.

1 Introduction

The MUSCL (Monotonic Upstream-centered Scheme for Conservation Laws) approach developed by Van Leer in a series of papers [1, 2], has become one of the most successful approaches to achieving higher-order accuracy in finite-volume methods. MUSCL refers to a comprehensive approach to achieving second- and higher-order accuracy in a finite-volume method with a monotonicity preserving mechanism designed for accurately capturing discontinuous solutions. In the MUSCL approach, a finite-volume discretization is constructed with cell-averaged solutions stored at cells as numerical solutions, where a higher order accurate flux is achieved at the cell face utilizing higher order accurate solutions reconstructed at the face from left and right cells using these numerical cell-averaged solutions. For the solution reconstruction, Van Leer proposed a one-parameter-family of solution reconstruction scheme, the κ -reconstruction scheme, where κ is a free parameter, and demonstrated that the finite-volume scheme can achieve third-order accuracy with $\kappa = 1/3$ [3, 4]. As one of the most important components of MUSCL being the solution reconstruction step, the word ‘‘MUSCL’’ is often used to mean the solution reconstruction. At the same time, ‘‘MUSCL’’ is also used for the resulting spatial finite-volume discretization: a finite-volume scheme constructed by the MUSCL approach is called a MUSCL scheme.

Despite its popularity over nearly four decades, there still exists some confusion about third-order accuracy of the MUSCL scheme as can be seen even in relatively recent papers. For example, it is claimed in Ref.[5] that the third-order MUSCL scheme is second-order accurate, which is then cited in Ref.[6]. In Refs.[7, 8], it is mentioned that an advection scheme based on the solution interpolation corresponding to $\kappa = 1/2$ is said to be third-order accurate, which implies that the MUSCL scheme with $\kappa = 1/3$ is not third-order, without any proof nor numerical verifications. In Ref.[9], the $\kappa = 1/3$ scheme is categorized as a second-order method, apparently on the assumption that the numerical solution is a point-valued solution; the MUSCL scheme has cell-averages as numerical solutions [1, 2]. Moreover, Ref.[10] claims to have proved that the MUSCL scheme cannot be third-order accurate for nonlinear equations. Later, this reference was cited as a proof of non-existence of third- and higher-order MUSCL schemes [11] and subsequently used as the basis for the development of low-dissipation schemes (rather than higher-order) as discussed in Refs.[12, 13]. Furthermore, Ref.[10] is still cited in a very recent reference [14] (2015) as a

*Associate Research Fellow (hiro@nianet.org)

proof of non-existence of third- and higher-order MUSCL schemes. In Ref.[15], the same reference [10] is cited and it is stated that for nonlinear equations, the MUSCL scheme is not third-order if the numerical solution is treated as a point value, but a higher-order scheme can be developed based on a direct flux extrapolation. The statement is true, but the scheme is no longer considered as a MUSCL scheme if the numerical solution is a point value (it is then a conservative finite-difference scheme [16]). Therefore, their statement is not true about the MUSCL scheme.

The truth is that the MUSCL scheme can have arbitrary high-order accuracy. In fact, over the last four decades, numerous high-order finite-volume schemes have been developed based on the MUSCL approach not only for Cartesian grids [17, 18, 19] but also for unstructured grids [20, 21, 22], just to name a few. A major reason for the confusion seems to lie in the fact that the truncation error analysis is not as straightforward for nonlinear equations as for linear equations. To the best of the author's knowledge, truncation error analyses of the MUSCL scheme applied to a nonlinear equation are found only in Refs.[23, 24] up to a second-order error, and in Ref.[10] up to a third-order error. Ref.[23] states that the MUSCL scheme can be third-order accurate with $\kappa = 1/3$ for steady linear and nonlinear conservation laws, but the MUSCL scheme is actually third-order with $\kappa = 1/3$ for a general nonlinear conservation law as we will show in this paper. More importantly, the proof presented in Ref.[10] is incomplete and their conclusion about the non-existence of a third-order MUSCL scheme is false. In proving third-order accuracy, one has to be very careful about the distinction between the point value and the cell average when expanding the scheme in the Taylor series (this distinction is not made in Refs.[10, 23]). Another important point missing in Refs.[10, 23] is that the operator approximated by the finite-volume scheme is not the point-valued flux derivative at a cell center but the cell-averaged flux derivative. Missing this point always leads to a second-order truncation error. There have been efforts already in the 1990's to clarify the correct orders of accuracy for various convection schemes [9, 25, 26, 27, 28] and the distinction between the point-valued and cell-averaged operators was recognized (especially by Leonard [9, 27, 28]), but analyses were performed only for linear convection equations and the numerical solution seems to have always been considered as a point value. In fact, schemes with point-valued numerical solutions are not MUSCL. As mentioned above (and will be further clarified in a subsequent paper), the MUSCL scheme will become a completely different scheme if used with the numerical solution is taken as a point value.

In this paper, we will provide a careful and detailed truncation error analysis of the MUSCL scheme applied to a nonlinear conservation law, and prove that the MUSCL scheme can achieve third-order accuracy with $\kappa = 1/3$. This paper is intended to serve as a reference to clarify the confusion about third-order accuracy of the MUSCL scheme and the choice of the diffusion scheme to preserve third-order accuracy, which is an important topic but has rarely discussed in the literature, and also as a guide to analyzing the MUSCL and related schemes for nonlinear equations. In order to minimize the chances of generating additional misunderstanding or confusion, we provide a full detail of each step in the truncation error analysis (which could be too much for a standard article) and thorough numerical studies to verify every claim deduced from the analysis and the definition of the MUSCL scheme.

Finally, we remark that there is a bigger motivation behind this work. Our ultimate goal is to clarify third-order unstructured-grid finite-volume schemes used in practical computational fluid dynamics solvers but largely confused in their mechanisms to achieve third- and possibly higher-order accuracy (e.g., third-order U-MUSCL with $\kappa = 1/2$ [29], $\kappa = 1/3$ [4], $\kappa = 0$ [30, 31]). The clarification is important for truly achieving third-order accuracy and taking full advantage of some economical third-order unstructured-grid schemes. In seeking the clarification, we have found that the confusion is largely rooted in the ever-present confusion over third-order convection schemes: the MUSCL scheme and the QUICK scheme [32]. This paper is the first paper in a series. The second paper will focus on the QUICK scheme.

The paper is organized as follows. In Section 2, we discuss the integral form of a nonlinear conservation law as a basis for a finite-volume discretization and point out the difference between the cell averaged and the point value solutions and operators. In Section 3, we describe the MUSCL scheme with the κ -reconstruction scheme applied to a nonlinear conservation law, and make it clear that the MUSCL scheme is based on cell-averaged solutions. In Section 4, we derive the truncation error of the MUSCL scheme and prove that third-order accuracy is achieved only with $\kappa = 1/3$. In Section 5, we derive a family of diffusion schemes compatible with the third-order MUSCL scheme. In Section 6, we present a series of numerical test results to verify the analysis and demonstrate third-order accuracy in the cell-averaged solution, not in the point-valued solution unless it is accurately recovered from the cell-averaged solution. In Section 7, we conclude the paper with final remarks.

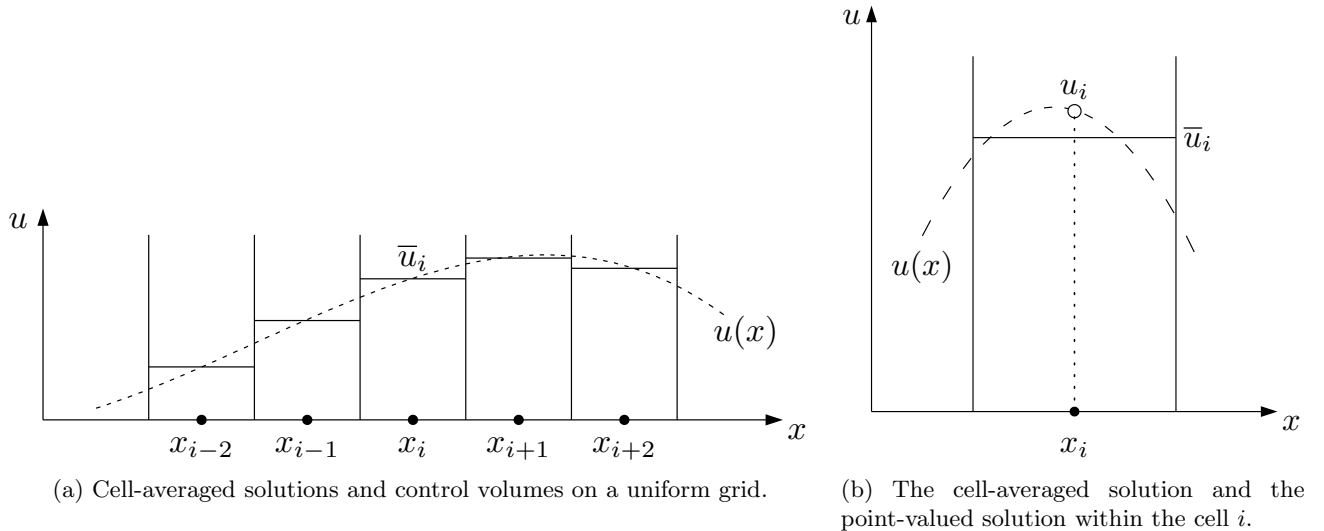


Figure 1: Cell-averaged solutions on a uniform grid and the comparison of the cell average and the point value in a cell i .

2 Exact Integral Form with Cell Average

Consider a one-dimensional conservation law in the differential form:

$$u_t + f_x = s(x), \quad (1)$$

where u is a solution variable, f is a flux and $s(x)$ is a forcing term, and the subscripts t and x denote the partial derivatives with respect to time and space, respectively. To derive an integral form, we consider a one-dimensional grid with a uniform spacing h : $x_{i+1} - x_i = h$, $i = 1, 2, 3, \dots, n$, where n is an integer. See Figure 1(a). In this paper, we focus on the interior of a domain and do not discuss any boundary effects. Then, we integrate the differential form (1) over a control volume around $x = x_i$, $x \in [x_{i-1/2}, x_{i+1/2}] = [x_i - h/2, x_i + h/2]$:

$$\int_{x_i-h/2}^{x_i+h/2} u_t dx + \int_{x_i-h/2}^{x_i+h/2} f_x dx = \int_{x_i-h/2}^{x_i+h/2} s(x) dx, \quad (2)$$

and obtain

$$\frac{d\bar{u}_i}{dt} + \frac{1}{h}[f(u_{i+1/2}) - f(u_{i-1/2})] = \bar{s}_i, \quad (3)$$

where \bar{u} and \bar{s} are the cell-averaged solution and forcing term:

$$\bar{u}_i = \frac{1}{h} \int_{x_i-h/2}^{x_i+h/2} u dx, \quad \bar{s}_i = \frac{1}{h} \int_{x_i-h/2}^{x_i+h/2} s(x) dx, \quad (4)$$

and $u_{i-1/2}$ and $u_{i+1/2}$ are the point-valued solutions at the left and right faces, respectively.

Note that the integral form is exact at this point and no approximation has yet been made. It thus represents the exact evolution equation for the cell-averaged solution \bar{u}_i . Then, a natural discretization approach is to store the cell-averaged solution at a cell as a numerical solution, compute the left and right fluxes with point-valued solutions reconstructed from the cell-averages, and then update the cell-averaged solution in time. This is the basis of the finite-volume method and the essence of the MUSCL approach of Van Leer for achieving second- and higher-order accuracy [1, 2]. Note also that it is absolutely clear already at this point from the exactness of the integral form that the MUSCL finite-volume method is arbitrarily high-order accurate with an arbitrarily high-order of solution reconstruction scheme. Therefore, the claim that the MUSCL scheme cannot be third-order [10] is false.

However, a confusion can easily arise when one attempts to prove third-order accuracy by a truncation error analysis for nonlinear equations. One of the main reasons is the lack of distinction of the cell-averaged solution \bar{u}_i and the point-valued solution $u_i = u(x_i)$, which differ by a second-order error (see Figure 1(b)):

$$\bar{u}_i = \frac{1}{h} \int_{x_i-h/2}^{x_i+h/2} u(x) dx = u_i + \frac{1}{24}(u_{xx})h^2 + O(h^4), \quad (5)$$

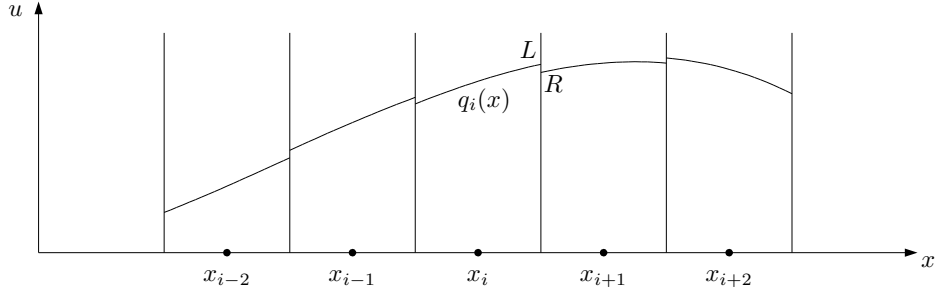


Figure 2: Quadratically reconstructed point-valued solution within each control volume on a uniform grid.

where $u(x)$ is a smooth solution that can be expanded around $x = x_i$ as

$$u(x) = u_i + (u_x)(x - x_i) + \frac{1}{2}(u_{xx})(x - x_i)^2 + \frac{1}{6}(\partial_{xxx}u)(x - x_i)^3 + \frac{1}{24}(\partial_{xxxx}u)(x - x_i)^4 + O(h^5). \quad (6)$$

Another important point that can be easily missed is that it is not the flux derivative f_x but the cell-averaged flux derivative $\overline{f_x}$ that the flux difference $[f(u_{i+1/2}) - f(u_{i-1/2})]/h$ represents:

$$\frac{d\overline{u}_i}{dt} + \overline{f_x} = \overline{s}_i, \quad (7)$$

where

$$\overline{f_x} = \frac{1}{h} \int_{x_{i-h/2}}^{x_{i+h/2}} f_x dx = \frac{1}{h} [f(u_{i+1/2}) - f(u_{i-1/2})]. \quad (8)$$

Therefore, the truncation error must be derived for the cell-averaged flux derivative $\overline{f_x}$, not the flux derivative f_x at a point. To clarify the confusion, we provide a detailed derivation of the third-order truncation error of the MUSCL scheme for a general nonlinear conservation law.

3 Third-Order MUSCL Scheme

3.1 Finite-volume discretization

On the one-dimensional grid defined in the previous section, we store the cell-averaged solution \overline{u}_i at a cell i as a numerical solution, and define a finite-volume scheme as the direct application of the integral form:

$$\frac{d\overline{u}_i}{dt} + \frac{1}{h} [F(u_{i+1/2,L}, u_{i+1/2,R}) - F(u_{i-1/2,L}, u_{i-1/2,R})] = \overline{s}_i, \quad (9)$$

where F denotes a numerical flux computed from two point-valued solutions reconstructed at a face, e.g., $u_{i+1/2,L}$ and $u_{i+1/2,R}$ at the right face. In this paper, we consider an upwind numerical flux in the form:

$$F(u_L, u_R) = \frac{1}{2} [f(u_L) + f(u_R)] - \frac{1}{2} D(u_R - u_L), \quad (10)$$

where D is a dissipation coefficient $D = |\partial f / \partial u|$, and u_L and u_R are reconstructed solutions at a face from the left and right cells, respectively. See Figure 2 for an example of piecewise quadratic polynomials reconstructed from the cell-averaged solutions. Here, we assume that the forcing term will be integrated exactly or by a sufficiently accurate quadrature formula. Then, the above discretization is exact if the reconstructed solutions are computed exactly; of course, they cannot be exact, and thus the solution reconstruction accuracy determines the order of accuracy of the finite-volume discretization.

3.2 Reconstruction scheme

For the solution reconstruction, we consider Van Leer's κ -reconstruction scheme, which first appeared in Ref.[3] and later was formulated specifically for a finite-volume discretization in Ref.[4]: for the right face at $i + 1/2$ (see

Figure 2),

$$u_L = \bar{u}_i + (u_x)_i \left(\frac{h}{2} \right) + \frac{3\kappa}{2} (u_{xx})_i \left[\left(\frac{h}{2} \right)^2 - \frac{h^2}{12} \right], \quad (11)$$

$$u_R = \bar{u}_{i+1} + (u_x)_{i+1} \left(-\frac{h}{2} \right) + \frac{3\kappa}{2} (u_{xx})_{i+1} \left[\left(-\frac{h}{2} \right)^2 - \frac{h^2}{12} \right], \quad (12)$$

where

$$(u_x)_i = \frac{\bar{u}_{i+1} - \bar{u}_{i-1}}{2h}, \quad (u_{xx})_i = \frac{\bar{u}_{i+1} - 2\bar{u}_i + \bar{u}_{i-1}}{h^2}, \quad (13)$$

$$(u_x)_{i+1} = \frac{\bar{u}_{i+2} - \bar{u}_i}{2h}, \quad (u_{xx})_{i+1} = \frac{\bar{u}_{i+2} - 2\bar{u}_{i+1} + \bar{u}_i}{h^2}, \quad (14)$$

or they can be simplified as

$$u_L = \frac{1}{2} (\bar{u}_i + \bar{u}_{i+1}) - \frac{1-\kappa}{4} (\bar{u}_{i+1} - 2\bar{u}_i + \bar{u}_{i-1}), \quad (15)$$

$$u_R = \frac{1}{2} (\bar{u}_{i+1} + \bar{u}_i) - \frac{1-\kappa}{4} (\bar{u}_{i+2} - 2\bar{u}_{i+1} + \bar{u}_i). \quad (16)$$

Note that we have denoted $u_{i-1/2,L}$ and $u_{i-1/2,R}$ simply as u_L and u_R for brevity; we consider only the right face across cells i and $i+1$ from now on since the left face is treated in a similar manner by shifting the index. Notice that the κ -reconstruction scheme has been generated from a local quadratic polynomial defined in each cell. For example, in the cell i shown in Figure 2, the quadratic polynomial $q_i(x)$ is given by

$$q_i(x) = \bar{u}_i + (u_x)_i (x - x_i) + \frac{1}{2} (u_{xx})_i \left[(x - x_i)^2 - \frac{h^2}{12} \right], \quad (17)$$

where

$$(u_x)_i = \frac{\bar{u}_{i+1} - \bar{u}_{i-1}}{2h}, \quad (u_{xx})_i = \frac{\bar{u}_{i+1} - 2\bar{u}_i + \bar{u}_{i-1}}{h^2}, \quad (18)$$

which gives u_L at $x = x_i + h/2$ as in Equation (11). It is important to note that this quadratic polynomial is a reconstruction of a point-valued solution from cell averages, which is clear from the fact that its cell-average is \bar{u}_i :

$$\frac{1}{h} \int_{x_i-h/2}^{x_i+h/2} q_i(x) dx = \bar{u}_i. \quad (19)$$

Note also that the derivatives $(u_x)_i$ and $(u_{xx})_i$ are point values as can be easily proved as

$$\left. \frac{dq_i(x)}{dx} \right|_{x=x_i} = (u_x)_i, \quad \left. \frac{d^2q_i(x)}{dx^2} \right|_{x=x_i} = (u_{xx})_i. \quad (20)$$

As pointed out in Ref.[4], the κ -reconstruction scheme corresponds to Fromm's scheme with $\kappa = 0$, a quadratic point-valued solution reconstruction (from cell averages) with $\kappa = 1/3$, a quadratic interpolation scheme (i.e., the QUICK interpolation scheme [32]) with $\kappa = 1/2$, and the central scheme with $\kappa = 1$. As we will show, third-order accuracy is achieved for the finite-volume scheme only with $\kappa = 1/3$.

Remark: Readers who are not familiar with the κ -reconstruction scheme written as in Equations (11) and (12) may find the following list of equivalent forms useful: Equations (11) and (12) are equivalent to

$$u_L = \bar{u}_i + \frac{1}{4} \{ (1-\kappa)\Delta_i^- + (1+\kappa)\Delta_i^+ \}, \quad u_R = \bar{u}_{i+1} - \frac{1}{4} \{ (1-\kappa)\Delta_{i+1}^+ + (1+\kappa)\Delta_{i+1}^- \}, \quad (21)$$

where

$$\Delta_i^- = \bar{u}_i - \bar{u}_{i-1}, \quad \Delta_i^+ = \bar{u}_{i+1} - \bar{u}_i, \quad (22)$$

which may be a convenient form to incorporate classical limiters [33, 34], or

$$u_L = \bar{u}_i + \frac{\kappa}{2}(\bar{u}_{i+1} - \bar{u}_i) + (1 - \kappa)(u_x)_i \frac{h}{2}, \quad u_R = \bar{u}_{i+1} - \frac{\kappa}{2}(\bar{u}_{i+1} - \bar{u}_i) - (1 - \kappa)(u_x)_{i+1} \frac{h}{2}, \quad (23)$$

which has been found useful for extending κ -reconstruction scheme to unstructured grids [11, 29], or

$$u_L = \kappa \frac{\bar{u}_i + \bar{u}_{i+1}}{2} + (1 - \kappa) \left[\bar{u}_j + \frac{1}{2}(u_x)_i h \right], \quad u_R = \kappa \frac{\bar{u}_{i+1} + \bar{u}_i}{2} + (1 - \kappa) \left[\bar{u}_{i+1} - \frac{1}{2}(u_x)_{i+1} h \right]. \quad (24)$$

which has been found useful for explaining how an unstructured-grid version of κ -reconstruction scheme can lose the linear exactness on unstructured grids [35]. Note also that the reconstruction scheme proposed in Ref.[11], which they call the β -scheme with a parameter β , is equivalent to the κ -reconstruction scheme with $\kappa = 1 - 2\beta$; thus it is a re-arrangement of the κ -reconstruction scheme. The scheme proposed in Ref.[36] is not equivalent but closely related to the κ -reconstruction scheme. With an additional term added, it is claimed to achieve third-order accuracy with $\kappa = -1/6$ for point-valued numerical solutions.

4 Accuracy of Third-Order MUSCL Scheme

To prove third-order accuracy of the MUSCL scheme with $\kappa = 1/3$, we first derive the so-called modified equation for the MUSCL scheme by expanding the numerical solution in a Taylor series [37]. Then, we identify the truncation error as the leading term in the difference between the modified equation and the target conservation law. For convenience, we will use the Taylor expansion of a point-valued solution and then take its cell-average to expand the cell-averaged solution.

In the rest of the section, we proceed as follows. First, we examine the accuracy of the solution reconstruction and show that the averaged solution at a face is exact for a cubic solution with $\kappa = 1/3$. Then, we prove that the same is true for the averaged flux term in the numerical flux (10); this is an important point for nonlinear equations. Furthermore, we will prove that the dissipation term in the numerical flux (10) is a fourth-order quantity at a face and therefore will only generate a third-order truncation error. Finally, we derive a modified equation of the MUSCL scheme by converting the resulting point-valued flux derivative to a cell-averaged derivative. Below, we will present as much detail as possible to leave no room for misunderstanding.

4.1 Accuracy of reconstruction

To examine the accuracy of the κ -reconstruction scheme, we consider a Taylor expansion of a smooth point-valued solution $u(x)$ around a cell center $x = x_i$:

$$u(x) = u_i + (u_x)(x - x_i) + \frac{1}{2}(u_{xx})(x - x_i)^2 + \frac{1}{6}(u_{xxx})(x - x_i)^3 + \frac{1}{24}(u_{xxxx})(x - x_i)^4 + O(h^5), \quad (25)$$

where u_i is a point value at $x = x_i$. It is very important to note here that the derivatives such as (u_x) and (u_{xx}) are also point values defined at $x = x_i$, which can be easily verified by differentiating $u(x)$ and evaluating the result at $x = x_i$. Here, we do not use the subscript i for the derivatives to distinguish them from the finite-difference approximations in Equations (13) and (14). It is possible and actually more convenient for our purpose to use a Taylor expansion of a cell-averaged solution with cell-averaged derivatives [19], but we do not employ such an approach here to illustrate and emphasize the importance of recognizing the difference between the cell average and the point value.

The exact reconstruction of a smooth solution at the right face is given by

$$u_{i+1/2}^{exact} = u(x_i + h/2) = u_i + \frac{1}{2}(u_x)h + \frac{1}{8}(u_{xx})h^2 + \frac{1}{48}(u_{xxx})h^3 + \frac{1}{384}(u_{xxxx})h^4 + O(h^5). \quad (26)$$

This is the target expression we wish to approximate as accurately as possible with the κ -reconstruction scheme. The κ -reconstruction scheme is expected to be exact up to the quadratic term since it is derived from a quadratic polynomial as discussed in the previous section, which is indeed true. To see this, we express (26) in terms of the cell-average stored at the cell i : take a cell-average of Equation (25),

$$\bar{u}_i = \frac{1}{h} \int_{x_i-h/2}^{x_i+h/2} u(x) dx = u_i + \frac{1}{24}(u_{xx})h^2 + \frac{1}{1920}(u_{xxxx})h^4 + O(h^6), \quad (27)$$

solve it for u_i , and substitute it into Equation (25) to get

$$u(x) = \bar{u}_i + (u_x)(x - x_i) + \frac{1}{2}(u_{xx}) \left[(x - x_i)^2 - \frac{h^2}{12} \right] + \frac{1}{6}(u_{xxx})(x - x_i)^3 + O(h^4), \quad (28)$$

which gives

$$u_{i+1/2}^{exact} = \bar{u}_i + (u_x) \frac{h}{2} + \frac{1}{2}(u_{xx}) \left[\left(\frac{h}{2} \right)^2 - \frac{h^2}{12} \right] + \frac{1}{6}(u_{xxx}) \left(\frac{h}{2} \right)^3 + O(h^4) \quad (29)$$

$$= \bar{u}_i + \frac{1}{2}(u_x)h + \frac{1}{12}(u_{xx})h^2 + \frac{1}{48}(u_{xxx})h^3 + O(h^4). \quad (30)$$

Comparing the κ -reconstruction scheme (11) with this exact expression, we find $\kappa = 1/3$ does produce the exact reconstruction up to the quadratic term. On uniform, however, it is actually exact up to the cubic term when u_L and u_R are averaged. This fact is pointed out in Ref.[38] by quoting Ref.[39], where a third-order finite-difference scheme is proposed, which is equivalent to the MUSCL scheme with $\kappa = 1/3$ for a linear advection equation (not for nonlinear equations).

Remark: The cubic exactness is a special property of a quadratically exact algorithm on a regular grid; the quadratic exactness is sufficient to design a third-order scheme on arbitrary grids. The resulting one-order higher truncation error is the reason that the truncation error order matches the discretization error (i.e., solution error) order on regular grids; the truncation error order is typically one-order lower on irregular grids. The MUSCL scheme can be made third-order on irregular grids by

$$u_{j+1/2} = \kappa \frac{\bar{u}_j + \bar{u}_{j+1}}{2} + (1 - \kappa) \left[\bar{u}_j + (u_x)_j \frac{h_R}{2} \right], \quad (31)$$

where $\kappa = 1/3$ and the gradient $(u_x)_j$ is computed exactly for a quadratic function by

$$(u_x)_j = \frac{h_L^2(\bar{u}_{j+1} - \bar{u}_j) + h_R^2(\bar{u}_j - \bar{u}_{j-1})}{h_L h_R (h_L + h_R)}, \quad h_L = x_j - x_{j-1}, \quad h_R = x_{j+1} - x_j, \quad (32)$$

which is exact for a quadratic function at a face halfway between x_j and x_{j+1} . See Refs.[40, 41, 42, 31] and references therein for further details about accuracy on irregular grids.

To prove the cubic exactness, we expand the κ -reconstruction schemes (11) and (12) by substituting the expansions of the cell-averages:

$$\bar{u}_{i-1} = \frac{1}{h} \int_{x_i-3h/2}^{x_i-h/2} u(x) dx = u_i - (\partial_x u)h + \frac{13}{24}(u_{xx})h^2 - \frac{5}{24}(u_{xxx})h^3 + O(h^4), \quad (33)$$

$$\bar{u}_i = \frac{1}{h} \int_{x_i-h/2}^{x_i+h/2} u(x) dx = u_i + \frac{1}{24}(u_{xx})h^2 + \frac{1}{1920}(\partial_{xxxx} u)h^4 + O(h^6), \quad (34)$$

$$\bar{u}_{i+1} = \frac{1}{h} \int_{x_i+h/2}^{x_i+3h/2} u(x) dx = u_i + (\partial_x u)h + \frac{13}{24}(u_{xx})h^2 + \frac{5}{24}(u_{xxx})h^3 + O(h^4), \quad (35)$$

$$\bar{u}_{i+2} = \frac{1}{h} \int_{x_i+3h/2}^{x_i+5h/2} u(x) dx = u_i + 2(\partial_x u)h + \frac{49}{24}(u_{xx})h^2 + \frac{17}{12}(u_{xxx})h^3 + O(h^4), \quad (36)$$

and obtain

$$u_L = u_i + \frac{1}{2}(u_x)h + \frac{1}{4}(u_{xx}) \left(\kappa + \frac{1}{6} \right) h^2 + \frac{5}{48}(u_{xxx})h^3 + \frac{60\kappa + 1}{1920}(u_{xxxx})h^4 + O(h^5),$$

$$u_R = u_i + \frac{1}{2}(u_x)h + \frac{1}{4}(u_{xx}) \left(\kappa + \frac{1}{6} \right) h^2 - \frac{1}{8} \left(\frac{7}{6} - 2\kappa \right) (u_{xxx})h^3 - \left(\frac{239}{1920} - \frac{5\kappa}{32} \right) (u_{xxxx})h^4 + O(h^5),$$

thus

$$\frac{u_L + u_R}{2} = u_i + \frac{1}{2}(u_x)h + \frac{1}{4}(u_{xx})\left(\kappa + \frac{1}{6}\right)h^2 - \frac{1}{8}\left(\frac{1}{6} - \kappa\right)(u_{xxx})h^3 - \frac{1}{16}\left(\frac{119}{120} - \frac{3\kappa}{2}\right)(u_{xxxx})h^4 + O(h^5), \quad (37)$$

which matches the exact reconstruction (26) up to the cubic term if

$$\kappa + \frac{1}{6} = \frac{1}{2}, \quad \frac{1}{6} - \kappa = -\frac{1}{6}, \quad (38)$$

both of which are satisfied with $\kappa = 1/3$, thus resulting in

$$\frac{u_L + u_R}{2} = u_i + \frac{1}{2}(u_x)h + \frac{1}{8}(u_{xx})h^2 + \frac{1}{48}(u_{xxx})h^3 - \frac{59}{1920}(u_{xxxx})h^4 + O(h^5). \quad (39)$$

Therefore, the κ -reconstruction scheme leads to the average of the reconstructed solutions exact for a cubic functions on a uniform grid. For a linear problem with $f = au$, where a is a constant, this means that the flux is reconstructed exactly for a cubic flux and thus it leads to a third-order MUSCL scheme for linear equations. However, for nonlinear equations, we must prove that the average of the nonlinear fluxes evaluated with the reconstructed solutions $[f(u_L) + f(u_R)]/2$ is also exact for a cubic flux. It requires a careful derivation as we will discuss in the next section.

4.2 Accuracy of flux

For nonlinear equations, the flux is a nonlinear function of u and thus it is not immediately clear if the averaged flux $[f(u_L) + f(u_R)]/2$ is also exact for a cubic flux. However, it is indeed exact for a cubic flux. To prove this, we will expand the averaged flux, but the expansion needs to be performed very carefully. Consider $f(u_L)$:

$$f(u_L) = f\left(\bar{u}_i + (u_x)_i\left(\frac{h}{2}\right) + \frac{3\kappa}{2}(u_{xx})_i\left[\left(\frac{h}{2}\right)^2 - \frac{h^2}{12}\right]\right), \quad (40)$$

which one might simply expand with respect to \bar{u}_i ,

$$f(u_L) = f(\bar{u}_i) + O((u_L - \bar{u}_i)^2). \quad (41)$$

However, we need a point-wise expansion of the flux around the cell center based on $f(u_i)$, not $f(\bar{u}_i)$, which differs by $O(h^2)$ and does not make sense. This is an important point because the flux derivatives arising from the flux expansion and to be used to represent the target equation in the modified equation should be point values, not those evaluated by the cell-averaged solution. The distinction is not made and it seems to be one of the major problems in the proof presented in Ref.[5]. To derive a correct truncation error, we write

$$f(u_L) = f(u_i + du), \quad du_L = u_L - u_i, \quad (42)$$

and expand it around the point value $f(u_i)$ as

$$f(u_L) = f(u_i) + (f_u)du_L + \frac{1}{2}(f_{uu})du_L^2 + \frac{1}{6}(f_{uuu})du_L^3 + O(du^4), \quad (43)$$

and similarly for $f(u_R)$,

$$f(u_R) = f(u_i) + (f_u)du_R + \frac{1}{2}(f_{uu})du_R^2 + \frac{1}{6}(f_{uuu})du_R^3 + O(du^4), \quad (44)$$

where $du_R = u_R - u_i$. Note that all the derivatives, e.g., (f_u) and (f_{uu}) , are point values at the cell center $x = x_i$. Then, we take the average to get

$$\begin{aligned} \frac{f(u_L) + f(u_R)}{2} &= f(u_i) + \frac{1}{2}(f_u)(u_x)h + \frac{1}{8}\left[\frac{6\kappa + 1}{3}(f_u)(u_{xx}) + (f_{uu})(u_x)^2\right]h^2 \\ &+ \frac{1}{48}\left[(f_{uuu})(u_x)^3 + (6\kappa + 1)(f_{uu})(\partial_x u)(u_{xx}) + (6\kappa - 1)(f_u)(\partial_{xxx} u)\right]h^3 + O(h^4). \end{aligned} \quad (45)$$

Comparing it with the exact flux reconstruction expressed in the Taylor series,

$$\begin{aligned}
f_{j+1/2}^{exact} &= f(u_i) + \frac{1}{2}(f_x)h + \frac{1}{8}(f_{xx})h^2 + \frac{1}{48}(f_{xxx})h^3 + O(h^4), \\
&= f(u_i) + \frac{1}{2}(f_{uu})(u_x)h + \frac{1}{8}[(f_u)(u_{xx}) + (f_{uu})(u_x)^2]h^2 \\
&+ \frac{1}{48}[(f_{uuu})(u_x)^3 + 3(f_{uu})(u_x)(u_{xx}) + (f_u)(u_{xxx})]h^3 + O(h^4),
\end{aligned} \tag{46}$$

we find that the averaged flux matches the exact flux up to the cubic term if

$$\frac{6\kappa + 1}{3} = 1, \quad 6\kappa + 1 = 3, \quad 6\kappa - 1 = 1, \tag{47}$$

which are all satisfied with $\kappa = 1/3$, thus giving

$$\begin{aligned}
\frac{f(u_L) + f(u_R)}{2} &= f(u_i) + \frac{1}{2}(f_u)(u_x)h + \frac{1}{8}[(f_u)(u_{xx}) + (f_{uu})(u_x)^2]h^2 \\
&+ \frac{1}{48}[(f_{uuu})(u_x)^3 + 3(f_{uu})(u_x)(u_{xx}) + (f_u)(u_{xxx})]h^3 + O(h^4).
\end{aligned} \tag{48}$$

Therefore, the average of the left and right fluxes evaluated with the solutions reconstructed with the κ -reconstruction scheme is exact for a cubic flux with $\kappa = 1/3$.

4.3 Order of dissipation

In this section, we show that the dissipation term is of $O(h^3)$ and does not contribute to the second-order truncation error. Consider the solution jump at the right face, which can be expanded by substituting the expanded cell-averages (33)-(36):

$$u_R - u_L = (\kappa - 1) \left[\frac{1}{4}(u_{xxx})h^3 + \frac{1}{8}(u_{xxxx})h^4 + O(h^5) \right]. \tag{49}$$

Observe that the jump vanishes for $\kappa = 1$ and it is consistent with the fact that $\kappa = 1$ corresponds to the central scheme, which has no dissipation. For a linear equation, the dissipation coefficient D in the upwind flux (10) is a global constant and the leading third-order term will cancel with the same term arising from the expansion of the jump from the left face. However, for nonlinear equations, the dissipation coefficient is generally a function of the solution. It is typically evaluated with the averaged solution:

$$D = D \left(\frac{u_L + u_R}{2} \right). \tag{50}$$

Note that other averages can be used but all differ from the arithmetic average by $O(u_R - u_L) = O(h^3)$, which is negligibly small for the purpose of our analysis. Hence, it suffices to consider the arithmetic average as in the above equation. This coefficient needs to be expanded as well in the truncation error analysis. In doing so, we assume that the dissipation coefficient is differentiable with a smoothing technique (e.g., see Ref.[43]) applied to the absolute value of the eigenvalue in constructing the absolute Jacobian $D = |\partial f / \partial u|$. Then, we expand the dissipation coefficient (50) by using Equation (39), and find

$$D = D(u_i) + \frac{1}{2}D_u(u_x)h + O(h^2). \tag{51}$$

where D_u is the derivative of D with respect to u at $x = x_i$. Therefore, the dissipation term at the right face is expanded as

$$D(u_R - u_L) = \left[D(u_i) + \frac{1}{2}D_u(u_x)h + O(h^2) \right] (\kappa - 1) \left[\frac{1}{4}(u_{xxx})h^3 + \frac{1}{8}(u_{xxxx})h^4 + O(h^5) \right] \tag{52}$$

$$= D(u_i) \frac{\kappa - 1}{4}(u_{xxx})h^3 + \frac{\kappa - 1}{8} [D_u(u_x)(u_{xxx}) + (u_{xxxx})] h^4 + O(h^5). \tag{53}$$

By performing a similar expansion for the dissipation term at the left face, we obtain exactly the same third-order leading term (and the same fourth-order term with the opposite sign). Therefore, the third-order contribution from the dissipation term will cancel out in the flux difference in Equation (9). Then, as the flux difference is divided by h , the leading error coming from the dissipation term will be $O(h^3)$. Hence, the truncation error of the dissipation in the MUSCL scheme is already sufficiently small for third-order accuracy. For this reason, we do not consider the dissipation term in the analysis below.

4.4 Accuracy of finite-volume scheme

We now derive the spatial truncation error of the MUSCL scheme by substituting the Taylor expansions of the fluxes and solutions as derived in the previous sections. Substituting the expansion of the averaged flux (45) at the right face and a similar expression for that at the left face, we obtain

$$\frac{d\bar{u}_i}{dt} + f_x + \frac{1}{24} [f_{uuu}(u_x)^3 + (6\kappa + 1) f_{uu}u_x u_{xx} + (6\kappa - 1) f_u u_{xxx}] h^2 + O(h^3) = \bar{s}_i, \quad (54)$$

where we have used $f_u u_x = f_x$, which is true since all derivatives are point values at $x = x_i$. There is a second-order error term, but the derivation is not completed yet. As mentioned earlier and repeatedly pointed out by Leonard [9, 28], the spatial operator that the finite-volume discretization is trying to approximate is not the pointwise f_x but the cell average \bar{f}_x . To derive a correct truncation error, we replace f_x by \bar{f}_x . Consider the cell-average of f_x .

$$\bar{f}_x = \frac{1}{h} \int_{x_i-h/2}^{x_i+h/2} f_x dx = f_x + \frac{1}{24} f_{xx} h^2 + \frac{1}{1920} f_{xxxx} h^4 + O(h^6), \quad (55)$$

from which we find

$$f_x = \bar{f}_x - \frac{1}{24} f_{xx} h^2 - \frac{1}{1920} f_{xxxx} h^4 - O(h^6), \quad (56)$$

and substituting this into Equation (54), we obtain

$$\frac{d\bar{u}_i}{dt} + \bar{f}_x + \frac{1}{24} [f_{uuu}(u_x)^3 + (6\kappa + 1) f_{uu}u_x u_{xx} + (6\kappa - 1) f_u u_{xxx} - f_{xxx}] h^2 + O(h^3) = \bar{s}_i, \quad (57)$$

which becomes by $f_{xxx} = f_{uuu}(u_x)^3 + 3f_{uu}u_x u_{xx} + f_u u_{xxx}$

$$\frac{d\bar{u}_i}{dt} + \bar{f}_x + \frac{3\kappa - 1}{12} [f_{uu}u_x u_{xx} + f_u u_{xxx}] h^2 + O(h^3) = \bar{s}_i. \quad (58)$$

Then, the second-order term vanishes for $\kappa = 1/3$:

$$\frac{d\bar{u}_i}{dt} + \bar{f}_x + O(h^3) = \bar{s}_i. \quad (59)$$

This is the correct modified equation for the third-order MUSCL scheme. By comparing with the target integral form (7), we find that the truncation error is $O(h^3)$. Therefore, the MUSCL scheme is third-order accurate with $\kappa = 1/3$ for a general nonlinear conservation law.

Note that we have just proved that the MUSCL scheme cannot be third-order with $\kappa = 1/2$. However, it does not disprove third-order accuracy of the QUICK scheme of Leonard [32] because the QUICK scheme is not equivalent to the $k = 1/2$ MUSCL scheme. It is still based on the integral form, but the numerical solution is taken as a point value, in which case the $\kappa = 1/3$ MUSCL scheme is not third-order accurate as analyzed in Ref.[9]. In a subsequent paper, we will provide a detailed discussion on the third-order QUICK scheme.

5 Fourth-Order MUSCL Diffusion Scheme

Before we move on to numerical experiments, we consider a MUSCL scheme for diffusion, which is required to solve a convection-diffusion equation:

$$f_x - \nu u_{xx} = 0, \quad (60)$$

where ν is a positive constant. This is an important subject but rarely discussed in the literature. To show its significance, we consider the following fourth-order diffusion scheme:

$$f_x - \nu \frac{-\bar{u}_{i-2} + 12\bar{u}_{i-1} - 22\bar{u}_i + 12\bar{u}_{i+1} - \bar{u}_{i+2}}{12h^2} = 0, \quad (61)$$

which is indeed fourth-order accurate as a finite-difference scheme,

$$f_x - \nu u_{xx} + \frac{37u_{xxxx}}{1920}h^4 + O(h^6) = 0, \quad (62)$$

but only second-order accurate as a finite-volume scheme approximating the integral form,

$$\frac{1}{h} \int_{x_i-h/2}^{x_i+h/2} f_x dx - \frac{1}{h} \int_{x_i-h/2}^{x_i+h/2} (\nu u_{xx}) dx + \frac{\nu}{24} (u_{xxxx})h^2 + O(h^4) = 0. \quad (63)$$

Therefore, if the third-order MUSCL scheme is used with this fourth-order diffusion scheme, the resulting scheme will be second-order accurate unless the diffusion term is negligibly small.

To construct a third-order MUSCL scheme for the convection-diffusion equation, we must construct a fourth-order finite-volume diffusion scheme. Consider the finite-volume discretization of the integral form of the diffusion term:

$$-\frac{1}{h} \int_{x_i-h/2}^{x_i+h/2} (\nu u_{xx}) dx \approx -\frac{1}{h} [F_{i+1/2}^d - F_{i-1/2}^d], \quad (64)$$

where F^d is the alpha-damping diffusive flux [44, 45],

$$F^d(u_L, u_R) = -\frac{1}{2} [\nu(u_x)_L + \nu(u_x)_R] + \frac{\nu\alpha}{2h} (u_R - u_L), \quad (65)$$

α is a constant damping coefficient to be determined later, and u_L , $(u_x)_L$, u_R , and $(u_x)_R$ are reconstructed point-valued solutions and derivatives at a face from the left and right cells, respectively. The left and right reconstructed solutions are evaluated by the κ -reconstruction scheme: Equations (15) and (16). As mentioned earlier, these solution values are evaluated by reconstructed quadratic polynomials, e.g., $q_i(x)$ given in Equation (17) for u_L . Then, it would be reasonable to compute $(u_x)_L$ by differentiating and evaluating $q_i(x)$:

$$(u_x)_L = \left. \frac{dq_i(x)}{dx} \right|_{x=x_i+h/2} = (u_x)_i = \frac{\bar{u}_{i+1} - \bar{u}_{i-1} + 3\kappa(\bar{u}_{i+1} - 2\bar{u}_i + \bar{u}_{i-1})}{2h}, \quad (66)$$

which becomes for $\kappa = 1/3$,

$$(u_x)_L = \frac{\bar{u}_{i+1} - \bar{u}_i}{h}. \quad (67)$$

Similarly, we find

$$(u_x)_R = \left. \frac{dq_{i+1}(x)}{dx} \right|_{x=x_{i+1}-h/2} = (u_x)_{i+1} = \frac{\bar{u}_{i+2} - \bar{u}_i + 3\kappa(\bar{u}_{i+2} - 2\bar{u}_{i+1} + \bar{u}_i)}{2h}. \quad (68)$$

which again becomes for $\kappa = 1/3$,

$$(u_x)_R = \frac{\bar{u}_{i+1} - \bar{u}_i}{h}. \quad (69)$$

Therefore, the derivative of the quadratic reconstruction is continuous across the face. Then, the diffusion scheme is given by

$$-\frac{\nu}{h} [F_{i+1/2}^d - F_{i-1/2}^d] = -\nu \frac{C_{i-2}\bar{u}_{i-2} + C_{i-1}\bar{u}_{i-1} + C_i\bar{u}_i + C_{i+1}\bar{u}_{i+1} + C_{i+2}\bar{u}_{i+2}}{h^2}, \quad (70)$$

where

$$C_{i-2} = C_{i+2} = \frac{1}{8} [\alpha(\kappa - 1) - 2(3\kappa - 1)], C_{i-1} = C_{i+1} = \frac{1}{8} [24\kappa - 4\alpha(\kappa - 1)], C_i = \frac{1}{8} [6\alpha(\kappa - 1) - 4(9\kappa + 1)], \quad (71)$$

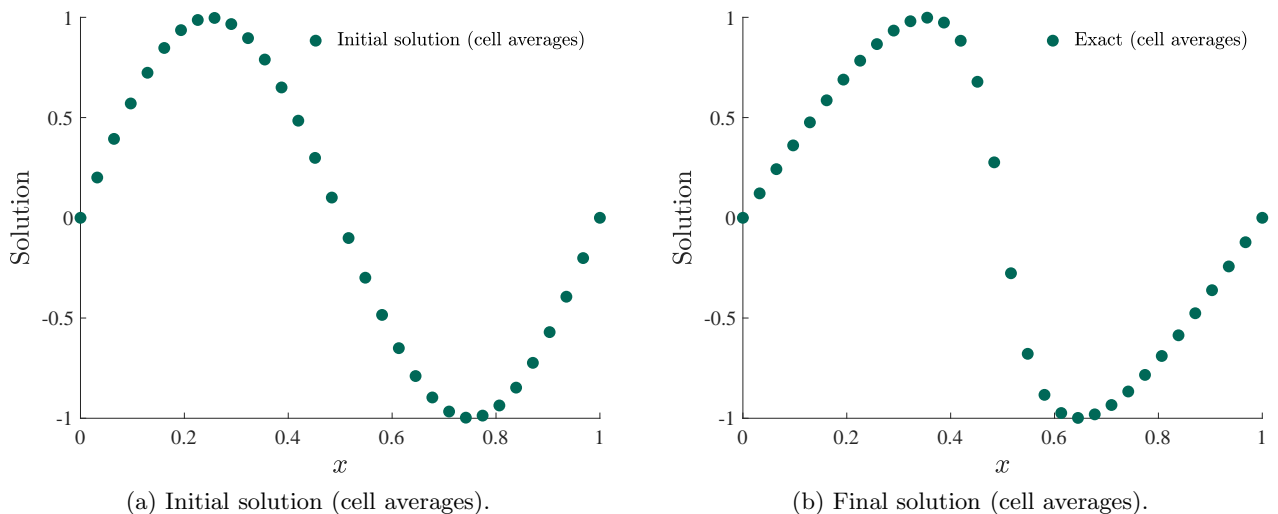


Figure 3: Initial and final solutions for the unsteady test case.

which can be expanded as

$$-\frac{\nu}{h} [F_{i+1/2}^d - F_{i-1/2}^d] = -\nu u_{xx} - \frac{1}{8} [\alpha(\kappa - 1) - 3(2\kappa - 1)] (\nu u_{xxxx}) h^2 + O(h^4), \quad (72)$$

thus leading to

$$-\frac{\nu}{h} [F_{i+1/2}^d - F_{i-1/2}^d] = \frac{1}{h} \int_{x_i-h/2}^{x_i+h/2} (\nu u_{xx}) dx - \frac{1}{8} \left[\alpha(\kappa - 1) - 3(2\kappa - 1) - \frac{1}{3} \right] (\nu u_{xxxx}) h^2 + O(h^4). \quad (73)$$

Therefore, to achieve fourth-order accuracy, we must set

$$\alpha(\kappa - 1) - 3(2\kappa - 1) - \frac{1}{3} = 0, \quad (74)$$

or

$$\alpha = \frac{2(4 - 9\kappa)}{3(1 - \kappa)}, \quad (75)$$

giving for $\kappa = 1/3$,

$$\alpha = 1 \quad (76)$$

Note that it gives $\alpha = 8/3$ for $\kappa = 0$, which is consistent with the value derived for fourth-order accuracy with $\kappa = 0$ in Refs.[44, 45]. Note also that the diffusion scheme (61) can be obtained with $\kappa = 1/3$ and $\alpha = 3/2$, which does not satisfy the condition (75). It is interesting to note that the fourth-order diffusion scheme compatible with the MUSCL scheme is unique as the substitution of Equation (75) into the scheme (71) gives

$$-\frac{1}{h} [F_{i+1/2}^d - F_{i-1/2}^d] = -\nu \frac{-u_{i-2} + 16u_{i-1} - 30u_i + 16u_{i+1} - u_{i+2}}{12h^2}. \quad (77)$$

This is the diffusion scheme required to achieve third-order accuracy for the convection-diffusion equation (60).

6 Numerical Results

6.1 Unsteady problem

We consider a time-dependent problem for Burgers's equation:

$$u_t + f_x = 0, \quad (78)$$

where $f = u^2/2$ in $x \in [0, 1]$ with the initial solution,

$$u(x) = \sin(2\pi x), \quad (79)$$

The domain is taken to be periodic (i.e., there is no boundary in this problem), and the solution is computed at the final time $t = t_f = 0.105$. The initial and final solutions are shown in Figure 3. The dissipation coefficient D is computed by the arithmetic average of the left and right values: $D = (|u_L| + |u_R|)/2$, which corresponds to the Roe linearization [46] with a smoothing technique of Harten and Hyman [43] applied to D . The time integration is performed by the three-stage SSP Runge-Kutta scheme [47] for the total of 840 time steps with a constant time step $\Delta t = 0.000125$, which has been found small enough for the discretization error (i.e., the error in the numerical solution) to be dominated by the spatial discretization. To verify the spatial order of accuracy, we performed computations with $\kappa = 0, 1/2$, and $1/3$ for a series of grids: 32, 64, 128, 256, 512, 1024, 2048 cells.

Note that the initial solution must be cell-averaged since the numerical solution is a cell average in the MUSCL scheme. Thus, we set at the beginning, for each cell i ,

$$\bar{u}_i = \frac{1}{h} \int_{x_i-h/2}^{x_i+h/2} \sin(2\pi x) dx = \frac{1}{2\pi h} [\cos(\pi(h-2x_i)) - \cos(\pi(h+2x_i))] = \frac{1}{\pi h} \sin(2\pi x_i) \sin(\pi h), \quad (80)$$

and then begin the time integration. The initial cell-averaged solution is plotted in Figure 3(a). Note that if the initial solution is given by the point value $\bar{u}_i = \sin(2\pi x_i)$, then a second-order error will be introduced immediately, even before we begin the time integration. Later, we will demonstrate this numerically.

To emphasize the difference between the cell average and the point value, we measure the discretization error in three different ways, locally at a cell i ,

$$\mathcal{E}_p(x_i) = |\bar{u}_i - u_{exact}(x_i, t_f)|, \quad \mathcal{E}_c(x_i) = \left| \bar{u}_i - \frac{1}{h} \int_{x_i-h/2}^{x_i+h/2} u_{exact}(x, t_f) dx \right|, \quad \hat{\mathcal{E}}_p(x_i) = |\hat{u}_i - u_{exact}(x_i, t_f)|, \quad (81)$$

where $u_{exact}(x, t_f)$ is the exact point-valued solution at the final time,

$$u_{exact}(x, t_f) = \sin(2\pi(x - u_{exact}t)), \quad (82)$$

which is defined implicitly and thus solved iteratively by the fix-point iteration (see Figure 3(b) for the final solution plotted on the coarsest grid), and \hat{u}_i is a point-valued solution at the cell center $x = x_i$ recovered from the cell-averaged solution \bar{u}_i as

$$\hat{u}_i = \bar{u}_i - \frac{1}{24} \left(\frac{\bar{u}_{i-1} - 2\bar{u}_i + \bar{u}_{i+1}}{h^2} \right) h^2, \quad (83)$$

which is an accurate representation of the point value at $x = x_i$ up to fourth-order and thus sufficiently accurate to verify third-order accuracy of the numerical solution. Finally, we define the discretization error by the L_1 norm:

$$L_1(\mathcal{E}_p) = \sum_{i=1}^n \frac{\mathcal{E}_p(x_i)}{n}, \quad L_1(\mathcal{E}_c) = \sum_{i=1}^n \frac{\mathcal{E}_c(x_i)}{n}, \quad L_1(\hat{\mathcal{E}}_p) = \sum_{i=1}^n \frac{\hat{\mathcal{E}}_p(x_i)}{n}, \quad (84)$$

where n is the number of cells in a grid.

Error convergence results are shown in Figure 4 for the case of cell-averaged initial solutions. As can be seen clearly in Figure 4(a), the numerical solution is third-order accurate as a cell-averaged solution with $\kappa = 1/3$ as expected. The choice $\kappa = 1/2$, which corresponds to the QUICK interpolation scheme, leads to second-order accuracy although slightly more accurate than Fromm's scheme ($\kappa = 0$). Figure 4(b) shows the result for the point-valued solution recovered from the cell-averaged solution as in Equation (83). Clearly, the recovered point-value solution is third-order accurate for $\kappa = 1/3$, but remains second-order accurate for the other choices. Finally, Figure 4(c) shows the error convergence for the pointwise error norm $L_1(\mathcal{E}_p)$. As expected, the numerical solution is second-order accurate as a point value for any κ .

To illustrate the importance of using cell-averaged initial solutions, we performed the same numerical experiments with point-valued initial solutions: $\bar{u}_i = \sin(2\pi x_i)$ at $t = 0$ for all cells, $i = 1, 2, 3, \dots, n$. Error convergence results are shown in Figure 5. As expected, the error is second-order for all error norms, indicating that the error is dominated by the initial second-order error committed in the initial solution. If we wish to avoid computing the

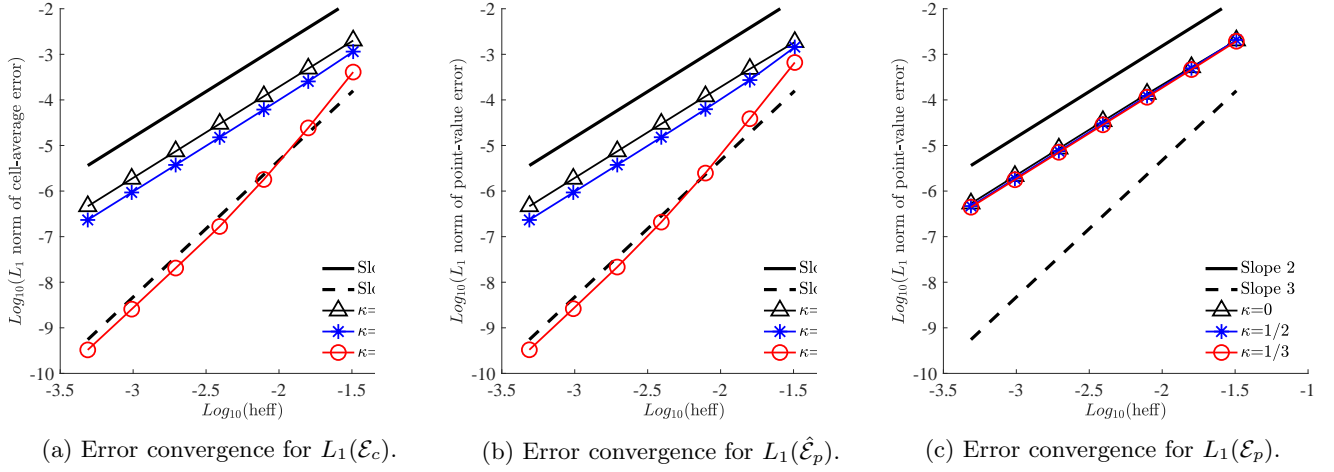


Figure 4: Error convergence results for the unsteady test case: cell-averaged initial solutions.

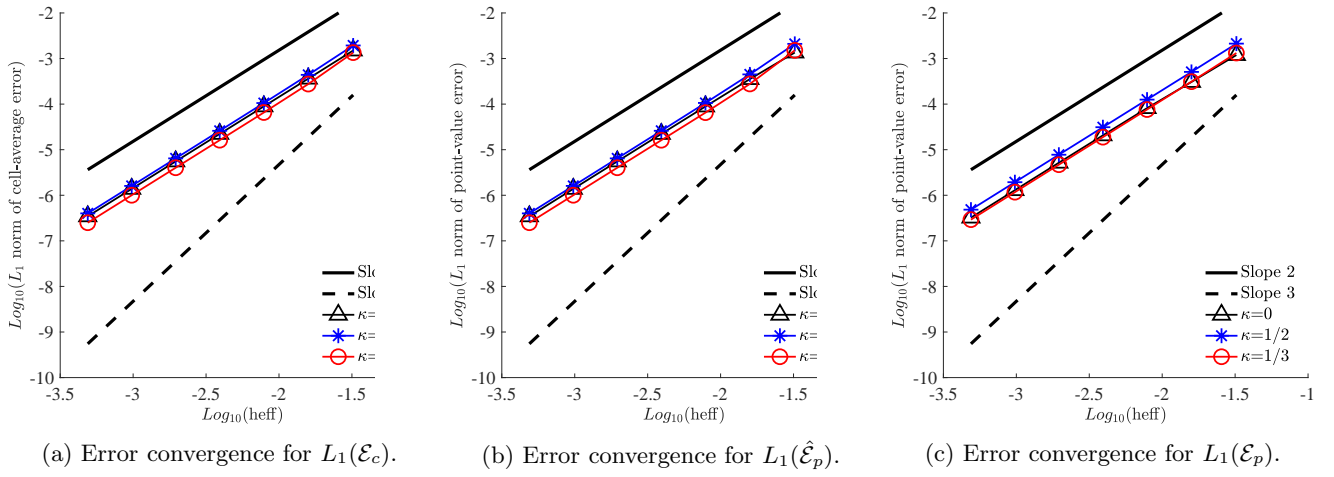


Figure 5: Error convergence results for the unsteady test case: point-valued initial solution

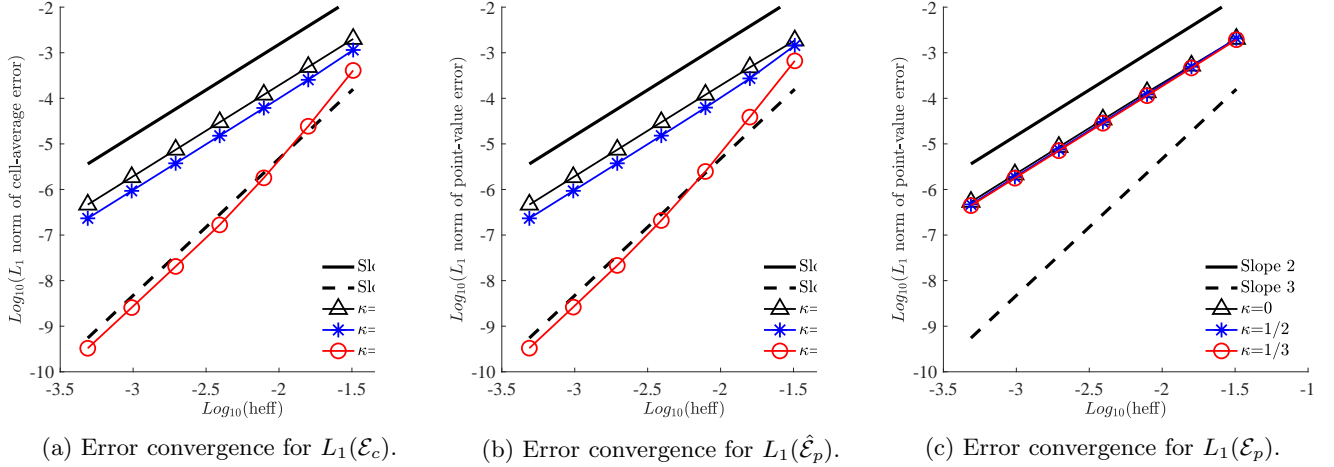


Figure 6: Error convergence results for the unsteady test case: corrected point-valued initial solution.

cell-averaged initial solution, we may compute a cell-averaged initial solution from a point-valued initial solution

with sufficient accuracy by

$$\bar{u}_i = u_i + \frac{1}{24} \left(\frac{u_{i-1} - 2u_i + u_{i+1}}{h^2} \right) h^2. \quad (85)$$

In this way, the initial solution does not need to be integrated over each cell. Results obtained with this correction are shown in Figure 6. As can be seen in Figures 6(a) and 6(b), third-order accuracy is achieved for the cell-averaged solution and the recovered point-value solution.

6.2 Steady convection problem

To demonstrate third-order accuracy for a convection equation with a forcing term, we consider a steady problem for Burgers's equation in $x \in [0, 1]$:

$$f_x = s(x), \quad (86)$$

where $f = u^2/2$, with the forcing term,

$$s(x) = 2 \sin(2x) \cos(2x), \quad (87)$$

so that the exact solution is given by

$$u(x) = \sin(2x). \quad (88)$$

For this problem, we drop the time-derivative term and define the residual at a cell i as

$$Res_i = \frac{1}{h} [F_{i+1/2}^c - F_{i-1/2}^c] - \bar{s}_i, \quad (89)$$

where the forcing term is exactly cell-averaged over each cell:

$$\bar{s}_i = \frac{1}{h} \int_{x_i-h/2}^{x_i+h/2} s(x) dx = \frac{1}{2h} [\cos^2(h-2x_i) - \cos^2(h+2x_i)]. \quad (90)$$

Then, we solve the system of nonlinear residual equations for the numerical solution: $\bar{u}_3, \bar{u}_4, \dots, \bar{u}_{n-3}, \bar{u}_{n-2}$. Note that we will provide the exact cell-averaged solutions at the left two cells $i = 1$ and 2 , and at the right cells $i = n-1$ and n , in order to exclude boundary effects, which are beyond the scope of the present study. An implicit solver based on the exact Jacobian of the first-order scheme is used to solve the residual equations. See Ref.[48], for example, for further details of the implicit solver for a one-dimensional finite-volume scheme. To verify the order of accuracy, we solve the steady problem over a series of grids with 15, 31, 63, 127 cells. As in the unsteady case, we consider two discretization error norms:

$$L_1(\mathcal{E}_p) = \frac{1}{n-4} \sum_{i=3}^{n-2} |\bar{u}_i - u_i^{exact}|, \quad L_1(\mathcal{E}_c) = \frac{1}{n-4} \sum_{i=3}^{n-2} |\bar{u}_i - \bar{u}_i^{exact}|, \quad (91)$$

where \bar{u}_i^{exact} is the exact cell-averaged solution:

$$\bar{u}_i^{exact} = \frac{1}{h} \int_{x_i-h/2}^{x_i+h/2} \sin(2x) dx = \frac{1}{2h} [\cos(h-2x_i) - \cos(h+2x_i)] = \frac{1}{2h} \sin(2x_i) \sin(h). \quad (92)$$

We also verify the order of truncation error numerically by substituting the exact solution into the residual (89), and taking the L_1 norm over the cells. We consider both the point-valued and cell-averaged solutions, and define the following two truncation error norms:

$$L_1(\mathcal{T}_p) = \frac{1}{n-4} \sum_{i=3}^{n-2} Res_i(\{u_i^{exact}\}), \quad L_1(\mathcal{T}_c) = \frac{1}{n-4} \sum_{i=3}^{n-2} Res_i(\{\bar{u}_i^{exact}\}), \quad (93)$$

where $Res_i(\{u_i^{exact}\})$ is the residual with the point-valued exact solution substituted, and $Res_i(\{\bar{u}_i^{exact}\})$ is the residual with the cell-averaged exact solution substituted,

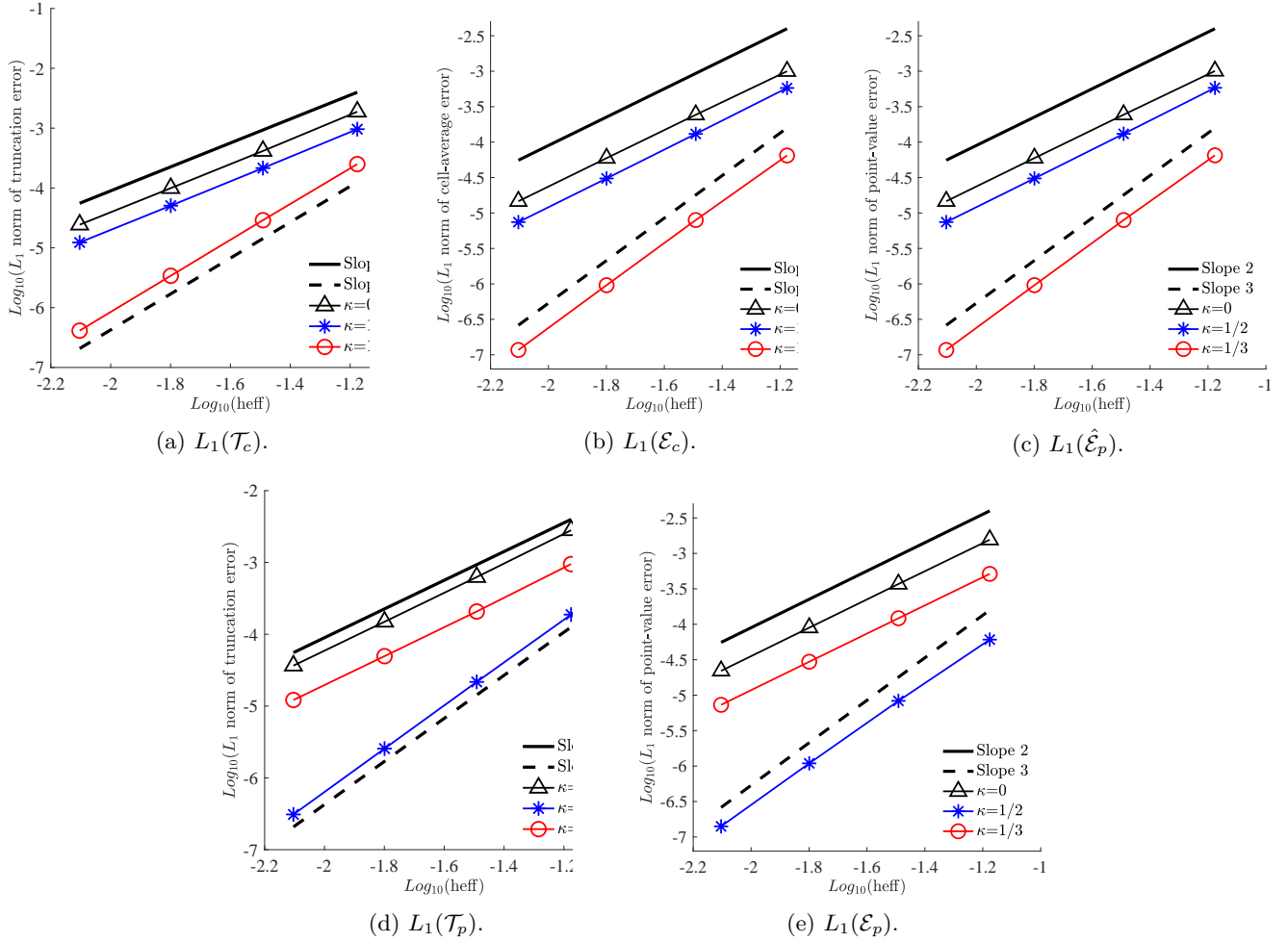


Figure 7: Truncation and discretization error convergence results for the case of the steady Burgers equation.

Error convergence results are shown in Figure 7. We first consider our target case, where the errors are measured with the exact cell-averaged solution. Figure 7(a) shows the truncation error convergence for $L_1(\mathcal{T}_c)$. As expected, it is third-order only with $\kappa = 1/3$. The discretization error is also third-order in both the cell-averaged solution and the recovered point-value solution. These results confirm our truncation error analysis.

On the other hand, if we compute the truncation error with the point-valued exact solution, we see third-order accuracy achieved with $\kappa = 1/2$ as shown in Figure 7(d). The same is observed for the discretization error. See Figure 7(e). To understand the result, we will need to clarify the QUICK scheme ($\kappa = 1/2$), which is planned in a subsequent paper. Therefore, here, we give only a short explanation. First of all, the numerical solution for a steady problem can be interpreted as either a point value or a cell average since it does not depend on an initial solution. Then, the flux balance term in the steady residual (89) is third-order with either combination: the $\kappa = 1/3$ quadratic reconstruction with cell-averaged solutions or the $\kappa = 1/2$ quadratic interpolation with point-valued solutions. The latter is the QUICK scheme of Leonard [32], as mentioned earlier; it is third-order for this steady convection equation with the cell-averaged forcing term. A further discussion on the QUICK scheme will be given in a subsequent paper. It is pointed out that third-order with $\kappa = 1/2$ is a special case and does not hold for a convection-diffusion problem, as we will discuss in the next section.

6.3 Steady convection-diffusion problem

To demonstrate the importance of the diffusion scheme, we consider a steady problem for the viscous Burgers equation with a forcing term:

$$f_x = \nu u_{xx} + s(x), \tag{94}$$

where $f = u^2/2$ and the forcing term is given by

$$s(x) = 2 \sin(2x) \cos(2x) + 4\nu \sin(2x), \quad (95)$$

so that the exact solution is given by

$$u(x) = \sin(2x). \quad (96)$$

Again, we integrate the forcing term is integrated exactly over each cell:

$$\bar{s}_i = \frac{1}{h} \int_{x_i-h/2}^{x_i+h/2} s(x) dx = \frac{1}{2h} [\cos^2(h-2x_i) - \cos^2(h+2x_i)] - \frac{2\nu}{h} [\cos(h-2x_i) - \cos(h+2x_i)]. \quad (97)$$

In particular, we consider the case $\nu = 1$, for which the convective and diffusion terms are equally important. As before, we solve the steady problem in $x \in [0, 1]$ by the implicit solver with $\kappa = 0, 1/2$, and $1/3$, for a series of grids with 15, 31, 63, 127 cells. The damping coefficient α is determined by Equation (75) for a given κ and the same u_L and u_R (i.e., the same κ) are used for both convective and diffusive fluxes. Note that u_L and u_R are used to compute the damping term in the diffusive flux. The analysis predicts that third-order accuracy is obtained only for $\kappa = 1/3$. To verify the analysis, we computed the truncation errors as well, and the discretization errors for both the cell-averaged and point-value exact solutions as described in the previous section.

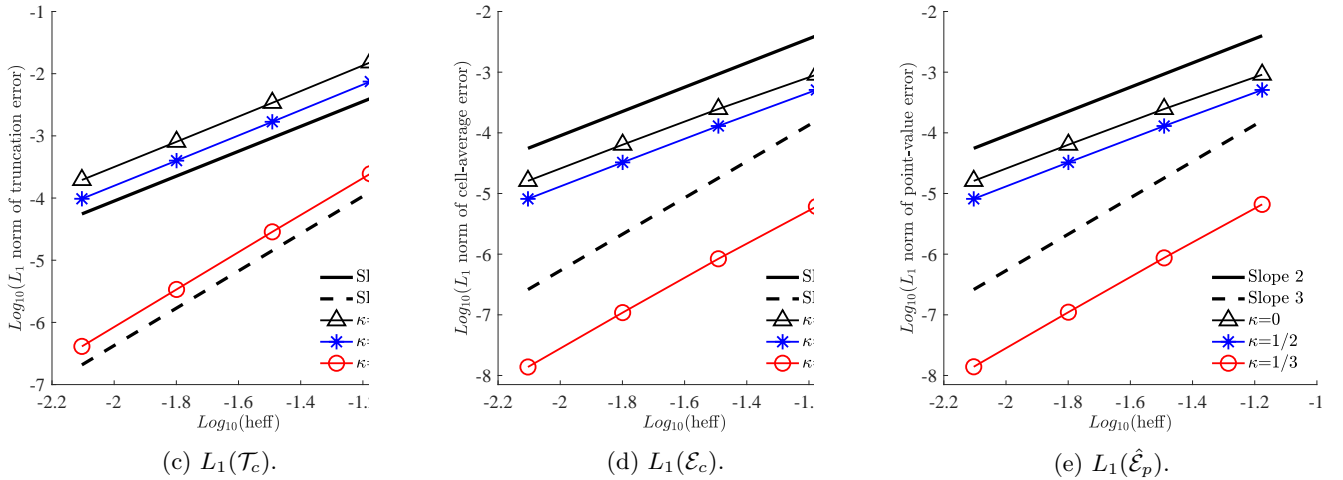
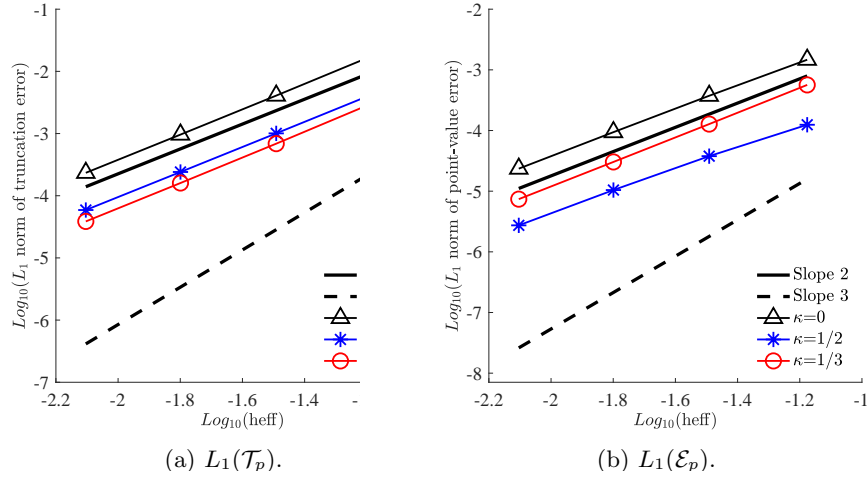


Figure 8: Truncation and discretization error convergence results for the case of the steady viscous Burgers equation. The fourth-order finite-volume diffusion scheme with $\alpha = \frac{2(4-9\kappa)}{3(1-\kappa)}$.

Figure 8 shows the results in terms of the point-value solution. As shown in Figure 8(a), the truncation error $L_1(\mathcal{T}_p)$ is second-order for all choices of κ . Figure 8(b) confirms that the discretization errors are also second-order

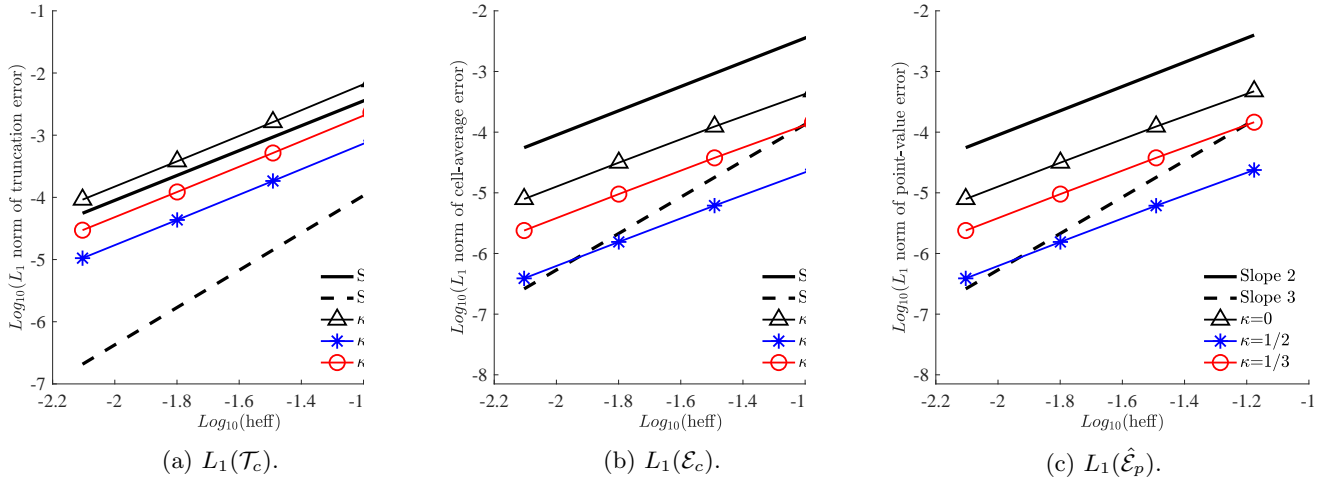


Figure 9: Truncation and discretization error convergence results for the case of the steady viscous Burgers equation. The fourth-order finite-difference diffusion scheme (61) implemented as the alpha-damping scheme with $\alpha = 3/2$.

for all choices of κ . Therefore, unlike the previous case, third-order accuracy is not achieved with $\kappa = 1/2$. This is because the use of the point-value solution changes the diffusion scheme whereas it does not affect the cell-averaged forcing term. As one can see, the condition (75) for fourth-order accuracy has been derived for the diffusion scheme (70) defined with the cell-averaged solutions. Once we replace the cell averages by the point values, the scheme involves the $O(h^2)$ error and loses fourth-order accuracy. Then, the resulting convection-diffusion scheme is second-order accurate at best unless the diffusion term is negligibly small compared with the convective term. Therefore, the choice of the diffusion scheme is critically important to achieve third-order accuracy.

On the other hand, the scheme is third-order with the cell-averaged solution. Figure 8(c) shows the truncation error convergence for $L_1(\mathcal{T}_c)$. As expected, the scheme achieves third-order accuracy with $\kappa = 1/3$. Also, third-order accuracy is confirmed in the discretization errors. See Figures 8(d) and 8(e).

Finally, we performed the computations with $\alpha = 3/2$, which corresponds to the incompatible diffusion scheme (61) when $\kappa = 1/3$. Results are shown in Figure 9. Clearly, as predicted in Section 5, third-order accuracy is never achieved. Therefore, it is very important to choose the right diffusion scheme in order to achieve third-order accuracy: the diffusion scheme must be a fourth-order finite-volume scheme with cell-averaged solution.

7 Conclusions

We have provided a detailed truncation error analysis and proved that the MUSCL scheme is third-order accurate with $\kappa = 1/3$ for a nonlinear conservation law. Two key points have been emphasized: (1) the distinction of the cell average and the point value in the Taylor expansion of the solution and flux, and (2) the target operator of the finite-volume discretization is the cell-averaged flux derivative, not the point value. It has been shown also that the κ -reconstruction scheme is exact for a cubic function on a uniform grid, when averaged across a face (i.e., averaging the reconstructed solutions at the left and right of the face), and the same is true for the average of the fluxes evaluated with the reconstructed solutions. The importance of the diffusion scheme is also discussed: third-order accuracy is lost with an incompatible four-order diffusion scheme. Third-order accuracy has been verified by numerical experiments for both unsteady and steady problems with Burgers' equation. For all the cases, it has been demonstrated that the MUSCL scheme gives third-order accurate cell-averaged solutions as well as third-order accurate point values at cell centers if the point values are accurately recovered from the third-order accurate cell averages. In a subsequent paper, we will discuss third-order accuracy of the QUICK scheme and clarify the reason that third-order accuracy was observed in the point value solution with $\kappa = 1/2$ for a steady problem.

Acknowledgments

The author is grateful to Emeritus Professor Bram van Leer for illuminating discussions and helpful suggestions. The author also would like to thank Jeffery A. White (NASA Langley Research Center) for valuable comments and discussions. The author gratefully acknowledges support from Software CRADLE, part of Hexagon, the U.S. Army

Research Office under the contract/grant number W911NF-19-1-0429 with Dr. Matthew Munson as the program manager, and the Hypersonic Technology Project, through the Hypersonic Airbreathing Propulsion Branch of the NASA Langley Research Center, under Contract No. 80LARC17C0004.

References

- [1] van Leer, B., “Towards the Ultimate Conservative Difference Scheme. IV. A New Approach to Numerical Convection,” *J. Comput. Phys.*, Vol. 23, 1977, pp. 276–299.
- [2] van Leer, B., “Towards the Ultimate Conservative Difference Scheme. V. A Second-Order Sequel to Godunov’s Method,” *J. Comput. Phys.*, Vol. 32, 1979, pp. 101–136.
- [3] van Leer, B., “Towards the Ultimate Conservative Difference Scheme. III. Upstream-centered Finite Difference Schemes for Ideal Compressible Flow,” *J. Comput. Phys.*, Vol. 23, 1977, pp. 263–275.
- [4] van Leer, B., “Upwind-Difference Methods for Aerodynamic Problems Governed by the Euler Equations,” *Fluid Mechanics, Lectures in Applied Mathematics*, Vol. 22, 1985, pp. 327–335.
- [5] Liu, M., “Computational study of convective-diffusive mixing in a microchannel mixer,” *Chemical Engineering Science*, Vol. 66, 2011.
- [6] Kresta, S. M., III, A. W. E., Dickey, D. S., and Atiemo-Obeng, V. A., editors, *Advances in Industrial Mixing: A Companion to the Handbook of Industrial Mixing*, John Wiley & Sons, 2015.
- [7] Song, B. and Amano, R. S., “A High-Order Bounded Discretization Scheme,” *Computational Fluid Dynamics and Heat Transfer: Emerging Topics*, edited by R. S. Amano and B. Sudén, WIT Press, 2011, pp. 3–5.
- [8] Zhang, D., Jiang, C., Liang, D., and Cheng, L., “A review on TVD schemes and a refined flux-limiter for steady-state calculations,” *J. Comput. Phys.*, Vol. 302, 2015.
- [9] Leonard, B. P. and Mokhtari, S., “Beyond First-Order Upwinding: The Ultra-Sharp Alternative for Non-Oscillatory Steady-State Simulation of Convection,” *Int. J. Numer. Meth. Fluids*, Vol. 30, 1990, pp. 729–766.
- [10] Wu, H., Wand, L., and Sun, G., “Non-Existence of Third Order MUSCL Schemes Unified Construction of ENO Schemes and a New Discontinuity Sharpening Technique - Stiff Source Term Approach,” *Computational Fluid Dynamics Review 1998*, 1998, pp. 300–317.
- [11] Debiez, C. and Dervieux, A., “Mixed-element-volume MUSCL methods with weak viscosity for steady and unsteady flow calculations,” *Comput. Fluids*, Vol. 29, 2000, pp. 89–118.
- [12] Abalakin, I. and A. Dervieux, T. A. K., “A vertex centered high order MUSCL scheme applying to linearised Euler acoustics,” INRIA Report, N 4459, April 2002.
- [13] Camarri, S., Salvetti, M. V., Koobus, B., and Dervieux, A., “A Low-Diffusion MUSCL Scheme for LES on Unstructured Grids,” *Comput. Fluids*, Vol. 33, 2004, pp. 1101–1129.
- [14] Abalakin, I., Bakhvalov, P., and Kozubskaya, T., “Edge-based reconstruction schemes for unstructured tetrahedral meshes,” *Int. J. Numer. Meth. Fluids*, Vol. 81, 2015, pp. 331–356.
- [15] Abalakin, I., Bakhvalov, P., and Kozubskaya, T., “Edge-Based Reconstruction Schemes for Prediction of Near Field Flow Region in Complex Aeroacoustics Problems,” *Int. J. Aeroacoust.*, Vol. 13, 2014, pp. 207–233.
- [16] Shu, C.-W. and Osher, S. J., “Efficient Implementation of Essentially Non-Oscillatory Shock-Capturing Schemes, II,” *J. Comput. Phys.*, Vol. 83, 1989, pp. 32–78.
- [17] Buchmüller, P. and Helzel, C., “Improved Accuracy of High-Order WENO Finite Volume Methods on Cartesian Grids,” *J. Sci. Comput.*, Vol. 61, 2014, pp. 343–368.
- [18] Buchmüller, P., Drehe, J., and Helzel, C., “Finite volume WENO methods for hyperbolic conservation laws on Cartesian grids with adaptive mesh refinement,” *Applied Mathematics and Computation*, Vol. 272, 2016, pp. 460–478.

- [19] Tamaki, Y. and Imamura, T., “Efficient dimension-by-dimension higher order finite-volume methods for a Cartesian grid with cell-based refinement,” *Comput. Fluids*, Vol. 144, 2017, pp. 74–85.
- [20] Barth, T. J. and Frederickson, P. O., “Higher Order Solution of the Euler Equations on Unstructured Grids using Quadratic Reconstruction,” AIAA Paper 90-0013, 1990.
- [21] Luo, H., Luo, L., Nourgaliev, R., Mousseau, V. A., and Dinhb, N., “A reconstructed discontinuous Galerkin method for the compressible Navier–Stokes equations on arbitrary grids,” *J. Comput. Phys.*, Vol. 229, 2010, pp. 6961–6978.
- [22] Jalali, A. and Ollivier-Gooch, C., “Higher-order unstructured finite volume RANS solution of turbulent compressible flows,” *Comput. Fluids*, Vol. 143, 2017, pp. 32–47.
- [23] Koren, B., “A Robust Upwind Discretization Method for Advection,” Report NM-R9308, April 1993.
- [24] Magolin, L. G. and Rider, W. J., “Numerical Regularization: The Numerical Analysis of Implicit Subgrid Models,” *Implicit Large Eddy Simulations: Computing Turbulent Fluid Dynamics*, edited by F. F. Grinstein, L. G. Magolin, and W. J. Rider, chap. 5, Cambridge University Press, Rhode-Saint-Genese, Belgium, 2006.
- [25] Johnson, R. W. and Mackinon, R. J., “Equivalent Versions of the QUICK Scheme for Finite-Difference and Finite-Volume Numerical Methods,” *Communications in Applied Numerical Methods*, Vol. 8, 1992, pp. 841–847.
- [26] Chen, Y. and Falconer, R. A., “Modified forms of the third-order convection, second-order diffusion scheme for the advection-diffusion equation,” *Advances in Water Resources*, Vol. 17, 1994, pp. 147–170.
- [27] Leonard, B. P., “Comparison of Truncation Error of Finite-Difference and Finite-Volume Formulations of Convection Terms,” *Appl. Math. Modell.*, Vol. 18, 1994, pp. 46–50.
- [28] Leonard, B. P., “Order of Accuracy of QUICK and Related Convection-Diffusion Schemes,” *Appl. Math. Modell.*, Vol. 19, 1995, pp. 644–653.
- [29] Burg, C. O. E., “Higher Order Variable Extrapolation for Unstructured Finite Volume RANS Flow Solvers,” AIAA Paper 2005-4999, 2005.
- [30] Katz, A. and Work, D., “High-Order Flux Correction/Finite Difference Schemes for Strand Grids,” *J. Comput. Phys.*, Vol. 282, 2015, pp. 360–380.
- [31] Nishikawa, H. and Liu, Y., “Accuracy-Preserving Source Term Quadrature for Third-Order Edge-Based Discretization,” *J. Comput. Phys.*, Vol. 344, 2017, pp. 595–622.
- [32] Leonard, B. P., “A Stable and Accurate Convective Modelling Procedure based on Quadratic Upstream Interpolation,” *Computer Methods in Applied Mechanics and Engineering*, Vol. 19, 1979, pp. 59–98.
- [33] Lynn, J. F., *Multigrid Solution of the Euler Equations with local preconditioning*, Ph.D. thesis, University of Michigan, Ann Arbor, Michigan, 1995.
- [34] Hirsch, C., *Numerical Computation of Internal and External Flows*, Vol. 2, A Wiley - Interscience Publications, 1990.
- [35] Nishikawa, H., “On the Loss and Recovery of Second-Order Accuracy with U-MUSCL,” *J. Comput. Phys.*, Vol. 417, 2020, pp. 109600.
- [36] Yang, H. Q. and Harris, R. E., “Development of Vertex-Centered High-Order Schemes and Implementation in FUN3D,” *AIAA J.*, Vol. 54, 2016, pp. 3742–3760.
- [37] Hirt, C. W., “Heuristic Stability Theory for Finite-Difference Equations,” *J. Comput. Phys.*, Vol. 2, 1968, pp. 339–355.
- [38] Waterson, N. P. and Deconinck, H., “Design principles for bounded higher-order convection schemes - a unified approach,” *J. Comput. Phys.*, Vol. 224, 2007, pp. 182–207.
- [39] Agarwal, R. K., “A Third-Order-Accurate Upwind Scheme for Navier-Stokes Solutions at High Reynolds Numbers,” Aiaa paper 81-0112, 1981.

- [40] Diskin, B. and Thomas, J. L., “Accuracy Analysis for Mixed-Element Finite-Volume Discretization Schemes,” *NIA Report No. 2007-08*, 2007.
- [41] Diskin, B. and Thomas, J. L., “Notes on accuracy of finite-volume discretization schemes on irregular grids,” *Appl. Numer. Math.*, Vol. 60, 2010, pp. 224–226.
- [42] Katz, A. and Sankaran, V., “Mesh Quality Effects on the Accuracy of CFD Solutions on Unstructured Meshes,” *J. Comput. Phys.*, Vol. 230, 2011, pp. 7670–7686.
- [43] Harten, A. and Hyman, J. M., “Self-Adjusting Grid Methods for One-Dimensional Hyperbolic Conservation Laws,” *J. Comput. Phys.*, Vol. 50, 1983, pp. 235–269.
- [44] Nishikawa, H., “Beyond Interface Gradient: A General Principle for Constructing Diffusion Schemes,” *Proc. of 40th AIAA Fluid Dynamics Conference and Exhibit*, AIAA Paper 2010-5093, Chicago, 2010.
- [45] Nishikawa, H., “Robust and Accurate Viscous Discretization via Upwind Scheme - I: Basic Principle,” *Comput. Fluids*, Vol. 49, No. 1, October 2011, pp. 62–86.
- [46] Roe, P. L., “Approximate Riemann Solvers, Parameter Vectors, and Difference Schemes,” *J. Comput. Phys.*, Vol. 43, 1981, pp. 357–372.
- [47] Gottlieb, S., Shu, C.-W., and Tadmor, E., “Strong Stability-Preserving High-Order Time Discretization Methods,” *SIAM Rev.*, Vol. 43, No. 1, 2001, pp. 89–112.
- [48] Nishikawa, H. and Liu, Y., “Hyperbolic Advection-Diffusion Schemes for High-Reynolds-Number Boundary-Layer Problems,” *J. Comput. Phys.*, Vol. 352, 2018, pp. 23–51.